Environ. Sci. Technol. **2008,** *42,* 5527–5533

A Structural Study of Cadmium Interaction with Aquatic Microorganisms

OLEG S. POKROVSKY,*,† GLEB S. POKROVSKI,† AND AGNES FEURTET-MAZEL‡

Laboratoire des Mécanismes et Transferts en Géologie (LMTG), UMR 5563, CNRS-OMP-Université Toulouse, 14 Avenue Edouard Belin, 31400 Toulouse, France, and Laboratoire d'Ecotoxicologie et d'Ecophysiologie des Systèmes Aquatiques (LEESA), UMR CNRS 5805, Université de Bordeaux 1, Place du Dr Peyneau, 33120 Arcachon, France

Received February 21, 2008. Revised manuscript received May 22, 2008. Accepted May 26, 2008.

The molecular mechanisms of cadmium toxicity for aquatic phototrophic microorganisms, reversible adsorption on the surface, and cellular uptake during growth were investigated by combining batch macroscopic experiments with atomic-level in situ Cd *K*-edge X-ray absorption fine structure spectroscopy. The following species were examined: marine planktonic (*Skeletonema costatum*, *Thalassiossira weissflogii*) and freshwater periphytic (*Navicula minima*, *Achnanthidium minutissum*) diatoms, cyanobacteria (*Gloeocapsa* sp.), anoxygenic phototrophic bacteria (*Rhodopseudomonas palustris*), and freshwater diatom-dominated biofilms. Upon short-term adsorption at the freshwater diatoms and cyanobacteria cell surface from a $NaNO_3$ or NaCl solution, Cd is octahedrally coordinated by oxygen at an average distance of 2.27 ± 0.02 Å and is associated with carboxylate groups. The atomic environment of cadmium incorporated into freshwater diatoms during long-term growth (operationally defined as Cd nonextracted by EDTA) is similar to that of adsorbed metal in terms of Cd−O first-shell distances and coordination numbers. Contrasting speciation is found for Cd incorporated into marine diatoms and adsorbed onto phototrophic anoxygenic bacteria *R. palustris*, where Cd is coordinated with three to five oxygen/nitrogen atoms and one to three sulfur atoms in the first atomic shell, likely in the form of cysteine/hystidine complexes or Cd−thiolate clusters. The Cd association with sulfhydryl groups in marine planktonic diatoms and anoxygenic bacteria is an important feature of Cd binding which can be useful for assessing the bioavailability of this metal.

Introduction

At the present time, serious concerns at the European level are raised regarding the pollution of French hydrosystems (Lot, Gironde) and estuaries of the Atlantic coast by various toxic metals (Zn, Pb, As, Hg, and, in particular, Cd) originating from industrial activity located in the middle part of the Lot River. Over the past 10 years, a group of geochemists and ecotoxicologists has been performing a thorough study of Cd migration, speciation, and biouptake along the pollution gradient in a pilot site of the Lot River basin down to the Gironde estuary in southwest France (e.g., refs *1–4*). Because the first step in metal uptake by biota is the adsorption of aqueous ions or complexes on external layers of the cell wall, the study of these "primary" adsorption processes is crucial for modeling the impact of aquatic organisms on metal transport in natural settings and the ecotoxicological consequences. In this study, we focus on Cd interactions with the first and most important biological component of trophic chains, the periphytic diatoms and photosynthetic bacteria grown under controlled laboratory conditions.

The molecular-level environment and speciation of metals such as zinc in diatom cultures have been recently characterized by X-ray absorption fine structure (XAFS) spectroscopy (*5*) combined with macroscopic and isotopic characterization (*6*). The present study is aimed at gaining further insight on metal speciation in diatom and other microorganism cultures by looking at another very important environmental pollutant, cadmium, which is often considered as biological analog of Zn, capable of substituting for Zn in some macromolecules and activating phytochelatin and glutathione production (*7*). A fairly large amount of data has been collected on the mechanisms of Cd toxicity for marine diatom cultures, Cd uptake, and its influence on their growth (*8*). Cadmium toxicity is usually explained by blocking and reducing the thiol sites on proteins. Similar to zinc and other metals, cadmium can interact with both high-affinity (phosphoryl, sulfhydryl) and low-affinity (carboxyl) sites on cell surfaces, depending on its concentration in solution. Rigorous analysis of these chemical processes requires, however, knowledge of the identity and molecular structure of metal complexes both on the surface and inside of the cells. Such information can be gained using *in situ* XAFS spectroscopy. For example, XAFS spectroscopy proved to be capable of distinguishing changes in the coordination and local environment of Cd attached to bacteria (*9, 10*) and on mineral surfaces (*11, 12*). However, determining the speciation of Cd associated with biological surfaces, notably at concentrations and biomass-to-metal ratios approaching those of the natural environment, remains unprecedented in the case of diatoms, their biofilms, and other phototrophic microorganisms.

The present study addresses several important open questions on the mechanisms of Cd interaction with aquatic biota: (1) Does the chemical status of reversibly adsorbed Cd depend on exposure time, pH, and its concentration in solution? (2) How can one relate Cd surface speciation inferred from a macroscopic thermodynamic approach with that directly observed by XAFS? (3) What is the difference in the chemical forms of cadmium adsorbed on the surface and incorporated inside the cells during their growth? (4) How specific is the Cd chemical environment between different diatom species, phototrophic bacteria, or natural biofilms? It is anticipated that answering these questions should provide a molecular-level basis for the quantitative and predictive modeling of Cd biogeochemical fluxes and their bioavailability in natural aquatic systems under various environmental conditions.

Materials and Methods

Monospecific cultures of marine planktonic *Skeletonema costatum* (SC), *Thalassiosira weisfloggi* (TW), and freshwater periphytic *Achnanthidium minutissimum* (AMIN) and *Navicula minima* (NMIN) diatoms were prepared as described previously (*6, 13*). Diatoms were cultured over 1−2 weeks to

* Corresponding author e-mail: oleg@lmtg.obs-mip.fr.
† CNRS-OMP-Université Toulouse.
‡ Université de Bordeaux 1.

10.1021/es800521a CCC: $40.75
Published on Web 07/01/2008

TABLE 1. Samples Used for XAFS Studies[a]

sample, new name	type of interaction	medium, conditions	duration of exposure	pH	$[Cd^{2+}]_{aq}$, μM (solution)	[Cd] in biomass, mmol/kg
AMIN-1	incorporation	Dauta, light	76 h	9.4	0.44[b]	4.5
AMIN-2	adsorption	0.01 M $NaNO_3$	30 min	7.78	4.4	106
NMIN-1	adsorption	0.01 M $NaNO_3$, dark	1 h	7.7	32	88
NMIN-2	adsorption	Dauta, dark	40 min	7.6	60	115
NMIN-3	adsorption	Dauta, light	3−5 min	6.55	2.3	7.2
NMIN-4	incorporation	0.1 M $NaNO_3$, light	24 h	6.95	8.8[b]	31
NMIN-5	incorporation	Dauta, light	77 h	8.16	9[c]	6.6
NMIN-6	incorporation	Dauta, light	120 h	8.2 ± 0.2	0.88 ± 0.26[b]	8.8
TW-1	adsorption	0.1 M $NaNO_3$, dark	72 h	7.68	53	26.5
TW-2	adsorption	0.7 M NaCl, dark	40 min	7.7	680	88
SC-1	adsorption	0.7 M NaCl, dark	40 min	8.66	442	53
SC-2	incorporation	f/2, light	72 h	8.61	9[c]	4.4−26.5
SC-3	adsorption	0.1 M $NaNO_3$, light	96 h	6.54	19	57.5
H_4SiO_4 silicic acid	adsorption	0.01 M $NaNO_3$	1 h	7.26	3600	133
SiO_2 vitreous SiO_2	adsorption	0.01 M $NaNO_3$	1 h	7.25	25	50
Gloeocapsa sp.	adsorption	0.1 M $NaNO_3$, dark	40 h	6.46	24	13
R. palustris	adsorption	0.01 M $NaNO_3$, dark	18 h	5.96	66	3.8
Biofilm-1	adsorption	0.01 M $NaNO_3$, dark	16 h	6.99	0.88	4.6
Biofilm-2	adsorption	0.01 M $NaNO_3$, dark	2 h	5.95	177	240

[a] All samples were freeze-dried prior the analysis. *Achnanthidium minutissimum* = AMIN; *Navicula minima* = NMIN; *Skeletonema costatum* = SC; *Thalassiosira weisflogii* = TW; 95 P = *Rhodopseudomonas palustris*; GI = *Gloeocapsa* sp. f-6gl. Dissolved organic carbon concentration in all samples was below 10 mg/L. All solutions were strongly undersaturated with respect to any individual solid phase of Cd. [b] The value was maintained constant within ±10−20% (unless indicated) by adding fresh nutrient solution in the course of growth, for Cd concentration in solution. [c] The initial Cd concentration in solution.

a concentration of ~10^7 cells/L at 20 °C in a sterile Dauta (freshwater) or f/2 (seawater) medium at pH ~7.6−8.2 under continuous aeration and harvested from the late exponential-stationary growth phase. Samples for adsorption experiments were grown in Cd-free media at $[Cd]_{tot} < 10^{-9}$ M. Samples for incorporation experiments (EDTA-nonextracted, see below) were grown under controlled Cd concentrations ($[Cd]_{tot} = 0.5-10$ μM), as verified by periodic sampling, Cd analysis, and aliquot addition, to keep the concentration constant (Table 1). Anoxygenic photosynthetic purple bacteria *Rhodopseudomonas palustris* (95-P) and mesophilic cyanobacteria *Gloeocapsa* sp. f-6gl were grown to the stationary phase on mineral Pfenning and D media, respectively (*14*). Natural biofilms were grown on glass supports deployed in the river channel for 2−4 weeks in the tributaries of the Lot River in southwestern France (Riou Viou and Riou Mort, refs *3, 4)*. The supports were colonized by 2-mm-thick biofilm composed of a compact association of different species of freshwater periphytic diatoms with <10% of bacteria, fungi, protozoa, their exudates, and mineral suspended matter. The biomass of live bacterial and diatom cells suspension and biofilms was quantified by its humid (centrifuged 25 min at 4500 g) and dry (lyophilized or freeze-dried) weights. Before the adsorption experiment, cells were rinsed three times in appropriate 0.01 M $NaNO_3$ or 0.7 M NaCl solution using centrifugation at 4500*g* (~500 mL of solution for 1 g of wet biomass) to remove, as possible, the adsorbed ions and organic cell exudates from the surface.

Cadmium adsorption experiments were designed to provide quantitative characterization of metal binding by the microorganism surface in a wide range of pH's and Cd(II) concentrations in solution. For this purpose, two types of experiments were performed: (*i*) adsorption at a constant initial cadmium concentration in solution as a function of pH (pH-dependent adsorption edge) and (*ii*) adsorption at a constant pH as a function of cadmium concentration in solution (adsorption isotherm). All solutions were undersaturated with respect to any solid cadmium oxide, hydroxide, or carbonate phase as verified by calculations using the MINTEQA2 computer code and corresponding database (*15*). Details of analytical and experimental procedures of Cd adsorption and verification of adsorption reversibility are provided in the Supporting Information (SI-1).

All investigated samples are listed in Table 1. The short-term adsorption experiments were performed as described in SI-1. The long-term growth samples result from culturing the cells in nutrient media with added Cd. For all growth (incorporation) experiments, prior to the analysis, the cells collected via centrifugation were rinsed in a proper electrolyte (Cd-free $NaNO_3$ or NaCl) and subsequently in a 0.01 M EDTA solution for 10 min in order to remove Cd that was reversibly adsorbed on most surface envelopes (e.g., refs *16–18)*. In this work, we will operationally define the intracellular metal as Cd not extracted by EDTA (see details in SI-1).

In all XAFS experiments, only freeze-dried biomass was used. The wet centrifuged biomass was submerged into liquid nitrogen and frozen at −80 °C before liophylization. Our previous study demonstrated identical chemical status of a metal such as Zn in wet cells and in freeze-dried samples (*5*); however, the latter allows a significantly higher concentration of metal without increasing the level of initial Cd loading and thus provides higher sensitivity for XAFS analysis.

XAFS spectra (including the X-ray absorption near-edge structure region or XANES, and the extended X-ray absorption fine structure region or EXAFS) of Cd-bearing solids, aqueous solutions, and freeze-dried cells were collected in the transmission or fluorescence mode (depending on Cd concentration) at the Cd *K* edge (~26.71 keV) over the energy range 26.3−27.6 keV on the BM29 bending-magnet beamline at the European Synchrotron Radiation Facility. Analysis of XAFS spectra (see below) of the same samples collected at ambient- and low-temperature conditions (e.g., NMIN-1, SC-1; see Table 2) yielded structural parameters identical within errors, demonstrating that structural disorder largely dominates over thermal motions in most microorganism samples and, thus, the temperature has no significant effect on the Cd atomic environment. The description of the XAFS reduction procedure can be found elsewhere (*5, 19*), and additional details about the data collection procedure are given in the Supporting Information (SI-2).

TABLE 2. Integral Structural Data on the Atomic Environment of Cd Adsorbed on or Incorporated by Microorganisms[a]

sample	E° (eV)	atom	N (atoms)	R (Å)	σ^2 (Å^2)	R factor
AMIN-1	26713.1	O	6.1 ± 1.1	2.26 ± 0.02	0.011 ± 0.004	0.017
AMIN-2	26713.7	O	6.5 ± 0.8	2.28 ± 0.01	0.009 ± 0.002	0.007
cryostat, 30 K		*C*	*1.5 ± 1.0*	*2.77 ± 0.05*	*0.008 f*	
		C/O	*1.5 f*	*3.08 ± 0.05*	*0.008 f*	
NMIN-1	26712.9	O	6.2 ± 1.0	2.27 ± 0.02	0.012 ± 0.003	0.015
		C	1.0 ± 0.3	2.7 ± 0.1	0.006 ± 0.003	
NMIN-1	26713.1	O	7.0 ± 1.5	2.29 ± 0.03	0.011 ± 0.003	0.010
cryostat, 30 K		C	1.1 ± 0.5	2.7 ± 0.1	0.004 ± 0.002	
NMIN-2	26712.6	O	5.5 ± 1.5	2.27 ± 0.02	0.011 ± 0.003	0.020
NMIN-3	26713.6	O	5.3 ± 0.8	2.26 ± 0.01	0.011 ± 0.002	0.007
NMIN-4	26713.2	O	6.1 ± 0.9	2.26 ± 0.01	0.010 ± 0.002	0.004
		P/Si	1.0 ± 0.5	3.38 ± 0.05	0.006 ± 0.002	
NMIN-5	26713.1	O	5.8 ± 0.8	2.27 ± 0.01	0.011 ± 0.002	0.007
NMIN-6	26713.0	O	5 ± 1.5	2.25 ± 0.02	0.010 ± 0.003	0.015
TW-1	26713.7	O	5.7 ± 0.7	2.26 ± 0.01	0.010 ± 0.002	0.004
TW-2	26713.1	O/N	3.5 ± 1.5	2.26 ± 0.05	0.012 ± 0.004	0.007
		Cl[b]	2.3 ± 1.0	2.54 ± 0.03	0.011 ± 0.003	
SC-1	26712.6	O/N	5.0 ± 1.0	2.29 ± 0.04	0.013 ± 0.004	0.006
		Cl[b]	1.2 ± 0.8	2.52 ± 0.02	0.007 f	
		P	1.0 ± 0.4	3.35 ± 0.05	0.008 f	
SC-1	26712.6	O/N	5.0 ± 1.0	2.30 ± 0.02	0.011 ± 0.003	0.005
cryostat, 30 K		Cl[b]	1.3 ± 0.4	2.53 ± 0.04	0.005 ± 0.002	
		P	0.9 ± 0.3	3.36 ± 0.03	0.008 f	
SC-2	26711.8	O/N	2.0 ± 1.0	2.32 ± 0.02	0.015 ± 0.003	0.0023
		S	3.0 ± 0.5	2.53 ± 0.02	0.007 ± 0.002	
SC-3	26712.6	O	7.0 ± 2.0	2.29 ± 0.02	0.015 ± 0.005	0.016
H_4SiO_4	26713.7	O	6.2 ± 0.7	2.26 ± 0.01	0.011 ± 0.003	0.0060
Cd ads. on H_4SiO_4		Si	0.9 ± 0.4	3.36 ± 0.04	0.010 ± 0.005	
SiO_2	26713.7	O	6.2 ± 0.6	2.28 ± 0.01	0.011 ± 0.002	0.011
Gloeocapsa sp.	26713.3	O	6.0 ± 1.5	2.26 ± 0.02	0.011 ± 0.003	0.010
95P−Cd	26712.6	O/N	3.5 ± 0.5	2.25 ± 0.01	0.010 ± 0.003	0.002
R. palustris		S	1.0 ± 0.3	2.53 ± 0.02	0.006 ± 0.002	
		P	0.7 ± 0.3	3.36 ± 0.04	0.008 f	
Biofilm-1	26713.1	O	6.5 ± 0.5	2.25 ± 0.01	0.013 ± 0.002	0.005
		C	1.2 ± 0.6	2.84 ± 0.05	0.008 f	
		P	1.3 ± 0.4	3.40 ± 0.03	0.008 f	
Biofilm-2	26713.7	O	6.8 ± 0.8	2.27 ± 0.01	0.010 ± 0.002	0.004
cryostat, 30 K		P	1.1 ± 0.3	3.44 ± 0.03	0.008 ± 0.003	
		C	*1.5 ± 0.5*	*2.7−3.0*	*0.007 f*	

[a] Samples were run at ambient temperature unless indicated. R = cadmium-backscatter mean distance, N = backscatter coordination number, σ^2 = squared Debye−Waller factor (relative to $\sigma^2 = 0$ adopted in the calculation of reference amplitude and phase functions by FEFF); R factor defines goodness of the total fit in R space as described in IFEFFIT (*35*), R factor < 0.02 means good fit; E° is the energy of the maximum of 1st edge derivative (±0.3 eV); f means that the parameter was fixed to the best value in the final EXAFS fit. Parameters *in italics* indicate that the indicated backscatter cannot be completely excluded, but its inclusion in the model leads to weak-to-negligible improvement of the fit statistics and quality. [b] Cl was preferred to S in the first Cd shell of SC-1 and TW-2 samples on the basis of XANES spectra (see Figure SI-1 and SI-3, Supporting Information) and sample preparation and treatment procedures (see text).

Results and Discussion

Adsorption Equilibria. The data for bacteria and freshwater biofilms were obtained at 25 °C and a constant ionic strength of 0.01 M $NaNO_3$, as a function of pH and Cd concentration. The concentration of adsorbed Cd as a function of equilibrium Cd concentration in solution ($[Cd^{2+}]_{aq}$) at pH 6.5−7.25 and the pH-dependent adsorption edge for cyanobacteria, anoxygenic phototrophic bacteria, and freshwater biofilms are presented in Figure 1a and b, respectively. At constant pH, the concentration of adsorbed Cd is proportional to $[Cd^{2+}]_{aq}$ over almost 3 orders of magnitude, suggesting a rouphly 1:1 stoichiometric interaction between Cd aqueous ions and the surface adsorption sites (Figure 1a). In all experiments, the total carboxylate group concentration is an order of magnitude higher than that of adsorbed Cd used for EXAFS measurements, as followed from the results of acid−base titrations of freshwater diatoms (*13*) and cyanobacteria (*20*). At constant $[Cd]_{total}$, a negligible adsorption of Cd is observed at pH < 3, an increase in adsorption occurs at 4 ≤ pH ≤ 7, and 100% adsorption on the surface is achieved at pH > 7−8 (Figure 1b).

Previous macroscopic and spectroscopic measurements suggest that the diatom cell wall structure can be viewed as a layer of amorphous silica (frustule) attached to a protein template from the interior of the cell and covered by a polysaccharide layer bearing negatively charged $>R-COO^-$ moieties (*13, 21*). Therefore, the metal speciation at the outermost diatom cell walls resulting from short-term adsorption is likely to be controlled by $>R-COO-Cd^+$ surface complexes, similar to Zn (*5, 6*), and solely carboxylate moieties were found to be sufficient to provide an adequate fit to the sorption data (*21*). Indeed, the order of Cd binding affinity to the diatoms' cell wall, *S. costatum* > *N. minima* > *A. minutissimum* > *T. weissflogii*, follows the trend established earlier for Zn (*6*), in agreement with the decrease of carboxylate group concentration in the surface layers (*13*).

Cd Chemical Status in Cultures. *Freshwater Diatoms, Cyanobacteria, and Their Biofilms.* XAFS spectra are shown in Figure 2, and derived structural parameters are listed in Table 2. XANES spectra of freshwater species, *A. minutissimum* (AMIN) and *N. minima* (NMIN), at a pH between 7 and 9 exhibit shapes and energy positions very close to those

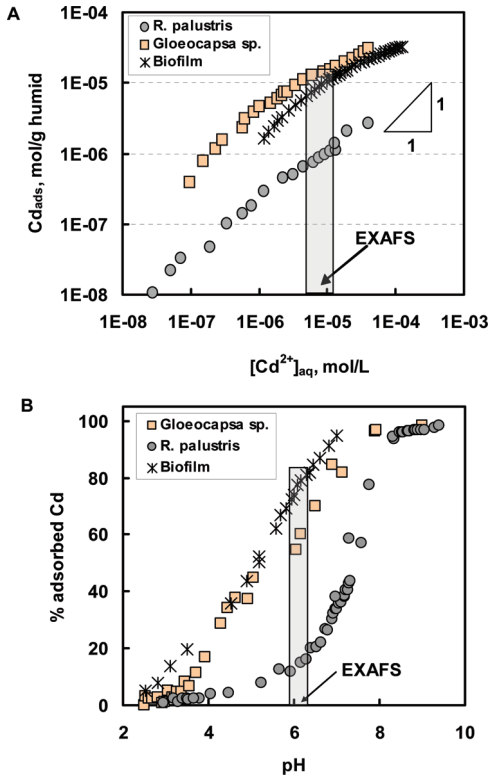

FIGURE 1. Results of cadmium adsorption onto microorganisms after 3 h exposure in the darkness. (A) Concentration of adsorbed Cd as a function of Cd concentration in solution. Experimental conditions: *R. palustris*, pH = 6.86, 10 g humid /L; *Gloeocapsa* sp., pH = 7.25, 4 g humid/L; Biofilm 1, pH = 6.53, 8.5 g humid/L. (B) Percentage of adsorbed Cd as a function of pH. Experimental conditions: *R. palustris*, $[Cd]_0 = 28\ \mu M$, 4 g humid /L; *Gloeocapsa* sp., $[Cd]_0 = 20\ \mu M$, 4 g humid/L; Biofilm 2, $[Cd]_0 = 20\ \mu M$, 4 g humid/L pH = 7.25, 4 g humid/L; Biofilm 1, $[Cd]_0 = 20\ \mu M$, 8.5 g humid/L. The shaded area corresponds to the region of EXAFS analysis.

of crystalline Cd acetate, oxalate, and citrate salts, and Cd nitrate and acetate aqueous solutions (Figure SI-1 of Supporting Information), suggesting an octahedral coordination for Cd^{2+}, likely with oxygen atoms. This is quantitatively confirmed by the EXAFS analysis showing that both adsorbed (samples NMIN-1, NMIN-2, NMIN-3, and AMIN-2) and incorporated (NMIN-4, NMIN-5, NMIN-6, and AMIN-1) cadmium is surrounded by 6 ± 1 oxygen/nitrogen atoms in the first coordination shell with Cd−O distances ranging from 2.25 to 2.28 Å (Table 2). The metal incorporated in the freshwater diatom cells during their growth exhibits similar, within errors, mean distances (2.26 ± 0.01 Å as averaged over the studied samples) as the reversibly adsorbed cadmium (2.27 ± 0.02 Å). Both types of samples exhibit EXAFS and FT amplitudes very similar to those of acetate solids and solutions (Figure 2, Table SI-3) but significantly lower than those of hydrated Cd^{2+} in an aqueous nitrate solution (Figure 2 and Figure SI-2) where Cd is surrounded by about six water molecules at ∼2.27 Å (see Table SI-1). The lower amplitude of the first-shell EXAFS signal in the organic samples in comparison to unbound hydrated Cd is quantitatively interpreted by the higher Debye−Waller factors ($\sigma^2 \sim 0.010-0.012$ Å^2 for ambient temperature samples, see Table 2), thus implying a larger disorder than that of aqueous Cd^{2+} ($\sigma^2 \sim 0.008$ Å^2, Table SI-1). Thus, although the mean values of the first-shell distances and numbers of neighbors are almost unaffected upon the uptake of Cd^{2+} from solution by the microorganisms, the increase of structural disorder indicates an inner-sphere binding of Cd to the cells, likely via Cd−O−C chemical linkages, in agreement with previous findings (*9*).

Note that, owing to the similarity of O and N backscatterer phases and amplitudes and Cd−O and Cd−N distances in most Cd−organic compounds, it was impossible to distinguish between these neighbors in the first coordination shell by EXAFS analysis. No first-shell splitting (i.e., the presence of two distinct subshells having different Cd−O/N distances), which might be indicative of the presence of different O- and N-binding groups, could be resolved in our samples, likely because of the limited spectral statistics (a minimal distance resolution for similar backscatterrers, $\Delta R = \pi/2\Delta k$, is ∼ 0.20 Å for most spectra). The Cd−O/N distances found in this study for diatom samples are in the range corresponding to Cd−O distances in cadmium oxalate, acetate, and citrate hydrated salts, in which Cd is typically coordinated to six O atoms from carboxylic groups both in mono- and bidendate fashion, and, eventually, water molecules (R_{Cd-O1} ∼ 2.23−2.35 Å, see Table SI-2 for details and literature references). At the same time, the first-shell distances of diatom samples are similar to those for Cd adsorbed on both hydrous and anhydrous amorphous silica ($SiO_2 \cdot nH_2O$ and SiO_2, vitreous, respectively), where Cd is found in a 6-fold coordination with oxygen at 2.26−2.28 Å (Table 2, samples H_4SiO_4−1 and SiO_2). For diatom cultures, our macroscopic measurements prove the dominance of organic (carboxylate-like from polysaccharide/protein layer) rather than inorganic (silanol from frustule) ligands in Cd binding by the diatom cell wall, as evidenced from a comparison of Cd adsorption on whole cells and isolated cell frustules ($SiO_2 \cdot nH_2O$), ref *21*. Therefore, although EXAFS allows both carboxylate and silanol binding, the first groups are most likely candidates for the Cd environment on diatoms' surfaces as follows from the surface complexation approach.

Second-shell features for Cd in most adsorption samples are too weak to allow the extraction of quantitative parameters from EXAFS fitting. Comparative analyses of the amplitudes, phases, and positions of these features for NMIN adsorbed samples (NMIN-1, NMIN-3) reveal some similarities with those in Cd acetate solids and solutions (Figure SI-2) in which Cd is bound to acetate ligand C_2-C_1OO via both oxygen atoms, resulting in a $Cd-C_1$ distance of ∼2.7 Å and a collinear multiple scattering feature $Cd-C_1-C_2$ from the C_2 atom in the acetate molecule, visible on the Fourier transform of some NMIN samples and Cd acetate solutions (Figure SI-1). This relatively short $Cd-C_1$ distance (2.7−2.8 Å) detected in some adsorbed samples (e.g., NMIN-1, AMIN-2) as compared to Cd−C distances in oxalate and citrate ($R_{Cd-C} \sim 3.0-3.2$ Å, see Supporting Information for literature references and full structural parameters), in which Cd is bound to one oxygen atom of the COO moiety, further confirm that Cd is likely to form bidentate linkages with both oxygen atoms of the COO ligand in the studied cultures. Similar structures were reported for Cd adsorbed on *Bacillus subtilis* bacterial cells (*9*). No other, heavier contributions like Cd−Cd, beyond the first atomic shells of adsorption samples, which could arise from Cd oxy(hydr)oxide polymers on the surface, were detected, in agreement with the undersaturation of all solutions with respect to Cd oxides and carbonate. Therefore, the EXAFS data allow a conclusion, based on the spectra similarities with Cd−acetate complexes and derived first- and second-shell structural parameters (e.g., samples NMIN-1, AMIN-2), that at least one or two water molecules in the first hydration sphere of Cd^{2+} are substituted by carboxylate groups on the cell surface, thus forming inner-sphere rather than outer-sphere complexes.

Second-shell features for the majority of incorporation samples of freshwater diatoms are also too weak to be resolved within the spectral statistics, with the only exception of NMIN-4 representing Cd incorporation during growth at

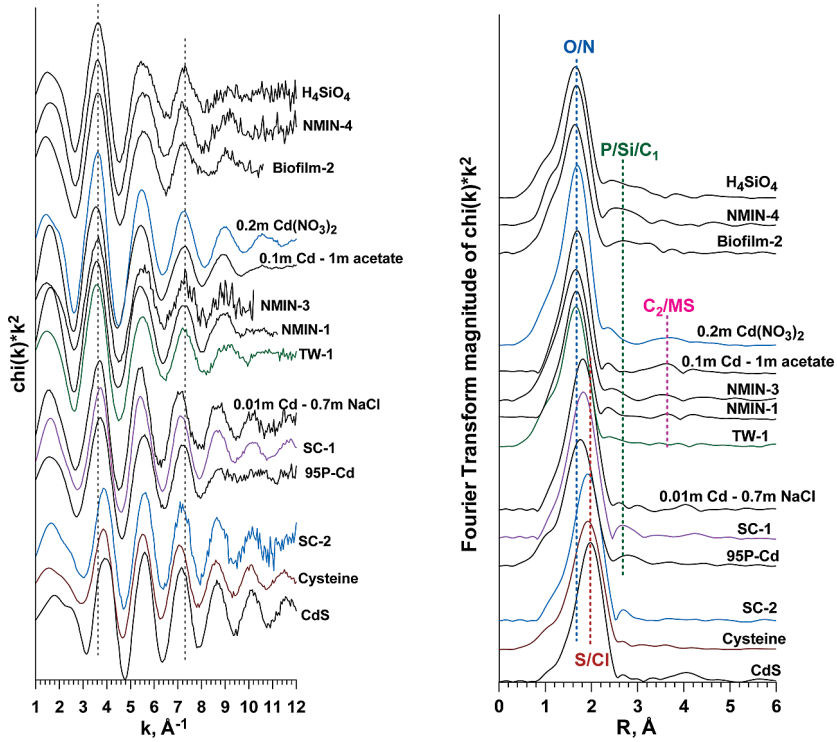

FIGURE 2. Normalized k^2-weighted EXAFS spectra at the Cd *K* edge of selected microorganism samples and reference solids and solutions (left), and their corresponding Fourier transform magnitude (right, FT transform *k* range = 2.1−10.0 Å^{-1}, Kaiser−Bessel window function with *dk* = 3.0; not corrected for phase shift). Vertical dashed lines on the left graph show changes in phase of EXAFS spectra depending on the dominant first shell backscattering atoms (O/N versus S/Cl) whereas those on the right graph denote approximate positions of different backscattering atoms around Cd (O, N, S, Cl, Si, P; C_1 and C_2 = first and second next-nearest carbon atoms; MS = linear multiple scattering path within the Cd−C_1−C_2 carboxyl moiety typical of Cd−acetate complexes). Spectra are shifted along the *y* axis for clarity.

neutral pH from a solution with $[Cd^{2+}]_{aq} = 8.8\,\mu$M. This sample has a pronounced second-shell feature which was modeled with 1 ± 0.5 P or Si atoms at ~3.38 Å from Cd. Similar Cd−P structures were also reported for Cd adsorbed on *B. subtilis* cells in acidic solutions (*9*) and on thermophilic *A. flavithermus* at pH > 7 (*10*). Note that these features are also very close to those found for Cd adsorbed on amorphous silica, with Cd−Si distances of 3.36 Å and coordination numbers close to 1 (sample H_4SiO_4, Table 2). Similarly to the failure of distinguishing between O and N in the first Cd shell (see above), it is impossible to distinguish, within the resolution of our measurements, the P of phosphoryl ligands inside the cell versus the Si of the cell walls as the major binding sites for incorporated cadmium in freshwater diatoms. However, it is known from literature data that the contribution of silica frustule to overall Cd binding by diatom cells is less than 10% (*21*), which is below the detection limits of our EXAFS analysis for Si second-shell neighbors (≤0.2 Si atoms). Therefore, within the resolution of EXAFS analysis, we submit Cd storage inside the freshwater diatom cells in the form of carboxylate and phosphoryl rather than silanol ligands. A similar conclusion has been reached for Zn interacting with diatom surfaces (*5*). Although the EXAFS data do not allow the resolution of stoichiometry of Cd binding to the surface carboxylates (bidentate mononuclear versus bidentate binuclear complexes), our macroscopic adsorption results suggest mononuclear rather than binuclear binding.

Two samples of natural biofilms having different Cd loadings (520 and 27 000 ppm) demonstrated the first shell of Cd to be consistent with 6O/N at 2.25−2.27 Å and likely the presence of P and C atoms in the second shell at ~3.4 and ~2.9 Å, respectively. This result corroborates our finding on freshwater diatoms that exhibit predominantly carboxylate group binding for Cd, with some eventual phosphoryl contribution.

The cadmium atomic environment described above was found to be independent of both the duration and level of exposure and the type of diatom species (AMIN or NMIN). This result is consistent with the surface complexation model of Cd interaction with diatom cell walls (*21*) and suggests that reversible adsorption of this metal on freshwater diatom surfaces is not likely to be coupled with cysteine-bearing ligands or Cd−histidine complex production; rather, the fixation of Cd on the outer polysaccharide matrix prevents its further uptake through the cell membrane. Therefore, we suggest that complexation with carboxylate surface groups is the primary process responsible for metal binding on *N. minima* cell walls. This corroborates results of previous investigations that have concluded that carboxyl and phosphoryl sites play dominant roles in metal biosorption by marine algae (*22*), bacteria (*10*), and bacterial Biofilm (*23*). NMR studies using ^{103}Cd also confirm the dominance of Cd−carboxylate complexes for algae and plant species, especially at high metal loadings (*24, 25*).

Marine Diatoms and Anoxygenic Photosynthesizing Bacteria. Samples resulted from the long-term adsorption of Cd onto marine (*S. costatum,* SC-3) and estuarine (*T. weissflogii,* TW-1) diatoms in 0.1 M $NaNO_3$ exhibit XANES spectra similar to those of Cd alginate, acetate, and freshwater NMIN species, thus suggesting the presence of oxygen in the first and probably carbon in the second coordination shells. EXAFS modeling is consistent with 6 ± 1 O at ~2.27 ± 0.02 Å in the first Cd atomic shell. Reversible short-term (~40 min) adsorption of Cd from 0.7 M NaCl solution on marine diatoms (samples TW-2 and SC-1) revealed the presence of about one to two Cl atoms originating from initial $CdCl_2$ salts in the NaCl media (see details of treatment in SI-2).

In contrast to adsorption samples, the long-term growth of *S. costatum* in the presence of a high Cd concentration (9 μM, sample SC-2) yields a shape and energy position of its

XANES spectrum very close to that of Cd cysteine (Figure SI-1). EXAFS modeling yields structural parameters that include ~4 ± 1 O/N atoms at 2.32 Å and 3.0 ± 0.5 S atoms at 2.53 Å, similar to Cd−cysteine (Table 2). This observation may be indicative of some detoxification mechanisms via phytochelatin production triggered by Cd incorporation in the cells (e.g., refs *26, 27)*. These ligands appear to play a role both in metal storage and in detoxification since low-level PC*n* concentrations are produced by many species of phytoplankton even at inorganic Cd contents far below those that impede the growth (*28, 29*). A recent study of freshwater biofilms exposed to different Cd concentrations did not demonstrate a straightforward increase in PC*n* with an increase of [Cd], likely because Cd-tolerant species produce less phytochelatin than Cd-sensitive ones (*17*). These observations may explain the lack of a Cd atomic environment change and the absence of S in the first shell of Cd incorporated in metal-tolerant freshwater diatoms *A. minutissimum* and *N. minima* compared to marine species *S. costatum*. Indeed, while the phytochelatin production by marine diatoms in response to metal stress is a well-established phenomenon, the quantitative characterization of phytochelatin production by freshwater diatoms, cyanobacteria, and phototrophic anoxygenic bacteria due to the presence of Cd in an external solution is largely unknown and should be a topic of future studies.

A particular environment of adsorbed Cd (O/N and S in the first shell, P in the second shell) is revealed in an anoxygenic phototrophic bacterium (*Rhodopseudomonas palustris*) where Cd binds on average with 3.5 ± 0.5 O/N and 1.0 ± 0.3 S in the first shell and 0.7 ± 0.3 P in the second shell, demonstrating the likely presence of phosphoryl ligands. Thus, the atomic environment of adsorbed Cd in *R. palustris* is different from Cd adsorbed on freshwater diatom *N. minima* but similar to Cd incorporated into marine diatom *S. costatum*. Note that the binding of Cd to S-bearing groups has been previously observed by EXAFS for Gram-negative bacterial surfaces *Shewanella oneidensis* (*30*), whereas Zn binding to sulfhydryl sites by heterotrophic Gram-negative bacteria is reported by Guiné et al. (*31*).

Comparisons of results of the present study with those of Zn adsorption and incorporation into diatoms demonstrate general similarities of Zn and Cd molecular interactions with phototrophic aquatic microorganisms. Both for freshwater diatoms and their biofilms, carboxylate binding is the main molecular environment for Zn and Cd. In contrast, upon adsorption and/or incorporation from an aqueous solution into diatoms, Zn changes its coordination from octahedral to tetrahedral (*5*), whereas Cd remains six-coordinated (this study). There are also differences in the main type of binding to C−COOH ligands. If $^{[6]}$Cd exhibits essentially bidentate linkages with the oxygens of carboxylate, $^{[4]}$Zn forms preferentially monodendate bonds with the hydroxyl group of the carboxyl ligand (*5*). The main reason for this difference is a larger size of the Cd ion (2.30 Å for $^{[6]}$Cd−O vs 2.00 Å for $^{[4]}$Zn−O), which allows the formation for Cd of stable chelate rings with oxygen−metal−oxygen angles close to 90°, whereas the tetrahedral coordination of the smaller Zn induces an angular distortion in the formed chelate which gives rise to strain energy and renders $^{[4]}$Zn chelates unstable. In the presence of larger and more covalent than O/N ligands, like thiols, Cd is likely to adopt a tetrahedral coordination, as it is found in Cd sulfide and cysteine (this study), and phylochelatine and synthetic peptide complexes (*32*).

Note that, at the high Cd concentrations used in this study to collect a sufficient EXAFS signal, it is inevitable that the majority of the Cd will be bound nonspecifically to the surface, perhaps masking the true physiological response of the cell to metal ions actually entering the cytoplasm. However, the typical metal-to-ligand ratio used in our experiments is 0.1−1 mg/L of Cd per 10 g/L of biomass. These ratios are not very far from what one can expect in natural settings, having 0.1−1 μg/L of dissolved Cd and 10−100 mg/L of biomass (10^6 to 10^7 cell/L, typical concentrations of plankton in natural waters). Our measurements are pertinent to the polluted site in the southwest of France (tributary of the Lot river). In this river, much higher Cd concentrations, between 10 and 40 μg/L in the dissolved phase and 100−500 mg/kg in the particulate, are reported throughout the year (*33*). This range of concentrations is consistent with the one used in the present study (e.g., Table 1, sample AMIN-1). The typical range of Cd concentration in polluted river biofilms is between 500 and 1000 mg/kg (*4, 34*). Therefore, knowledge of the atomic environment of adsorbed and incorporated cadmium gained in the present study will help to identify the structural factors controlling the Cd toxicity for autotrophic organisms. Such a molecular-level understanding will be the key to establishing a sound scientific basis for determining the quality status of water reservoirs and for developing reliable predictive models of the impact of pollutants on aquatic ecosystems.

Acknowledgments

We thank four anonymous reviewers and the Associate Editor Dr. L. Sigg for constructive reviews. The work was supported by French National Programs for Basic Research (EC2CO), Ecosphère Continentale et Côtière. We are indebted to O. Mathon for his assistance during XAFS experiments. We thank the ESRF committee Surfaces & Interfaces for providing beam time and access to the synchrotron facility.

Supporting Information Available

Chemical analyses, adsorption procedure, EDTA treatment of incorporation samples, and adsorption reversibility tests are given in SI-1. Details of the EXAFS spectra collection and reduction procedure, XANES spectra of investigated samples, and imaginary part of the Fourier transform of EXAFS spectra of selected microorganisms samples and reference compounds are presented in SI-2.This material is available free of charge via the Internet at http://pubs.acs.org.

Literature Cited

(1) Andrès, S.; Baudrimont, M.; Lapaquellerie, Y.; Ribeyre, F.; Maillet, N.; Latouche, C.; Boudou, A. Field transplantation of the freshwater bivalve *Corbicula fluminea* along a polymetallic contamination gradient (river Lot, France) - Part I: Geochemical characteristics of the sampling sites and cadmium and zinc bioaccumulation kinetics. *Environ. Toxicol. Chem.* **1999**, *18*, 2462–2471.

(2) Gold, C.; Feurtet-Mazel, A.; Coste, M.; Boudou, A. Impacts of metals (Cd, Zn) on the development of periphytic diatom communities within outdoor artificial streams along a pollution gradient. *Arch. Environ. Toxicol.* **2003**, *44*, 189–197.

(3) Morin, S.; Duong, T. T.; Dabrin, A.; Coynel, A.; Herlory, O.; Baudrimont, M.; Delmas, F.; Durrieu, G.; Schäfer, J.; Winterton, P.; Blanc, G.; Coste, M. Long-term survey of heavy-metal pollution, Biofilm contamination and diatom community structure in the Riou Mort watershed, South-West France. *Environ. Pollut.* **2008**, *151*, 532–542.

(4) Morin, S.; Vivas-Noguès, M.; Duong, T. T.; Boudou, A.; Coste, M.; Delmas, F. Dynamics of benthic diatom colonization in a cadmium/Zinc-polluted river (Riou-Mort, France). *Fundam. Appl. Limnol.* **2007**, *168*, 179–187.

(5) Pokrovsky, O. S.; Pokrovski, G. S.; Gélabert, A.; Schott, J.; Boudou, A. Speciation of Zn associated with diatoms using X-ray Absorption Spectroscopy. *Environ. Sci. Technol.* **2005**, *39*, 4490–4498.

(6) Gélabert, A.; Pokrovsky, O. S.; Viers, J.; Schott, J.; Boudou, A.; Feurtet-Mazel, A. Interaction between zinc and freshwater and marine diatom species: Surface complexation and Zn isotope fractionation. *Geochim. Cosmochim. Acta* **2006**, *70*, 839–857.

(7) Lane, T. W.; Saito, M. A.; George, G. N.; Pickering, I. J.; Prince, R. C.; Morel, F. M. M. A cadmium enzyme from a marine diatom. *Nature* **2005**, *435*, 42.

(8) Phinney, J. T.; Bruland, K. W. Uptake of lipophilic organic Cu, Cd, and Pb complexes in the coastal diatom *Thalassiosira weissflogii*. *Environ. Sci. Technol.* **1994**, *28*, 1781–1790.
(9) Boyanov, M. I.; Kelly, S. D.; Kemner, K. M.; Bunker, B. A.; Fein, J. B.; Fowle, D. A. Adsorption of cadmium to *Bacillus subtilis* bacterial cell walls: A pH-dependent X-ray absorption fine structure spectroscopy study. *Geochim. Cosmochim. Acta* **2003**, *67*, 3299–3311.
(10) Burnett, P-G. G.; Daughney, C. J.; Peak, D. Cd adsorption onto *Anoxybacillus flavithermus*: Surface complexation modeling and spectroscopic investigations. *Geochim. Cosmochim. Acta* **2006**, *70*, 5253–5269.
(11) Spadini, L.; Manceau, A.; Schindler, P. W.; Charlet, L. Structure and stability of Cd^{2+} surface complexes on ferric oxides. 1. Results from EXAFS Spectroscopy. *J. Colloid Interface Sci.* **1994**, *168*, 73–86.
(12) Randall, S. R.; Sherman, D. M.; Ragnarsdottir, K. V.; Clare, R. The mechanism of cadmium surface complexation on iron oxyhydroxide minerals. *Geochim. Cosmochim. Acta* **1999**, *63*, 2971–2987.
(13) Gélabert, A.; Pokrovsky, O. S.; Schott, J.; Boudou, A.; Feurtet-Mazel, A.; Mielczarski, J.; Mielczarski, E.; Mesmer-Dudons, N.; Spalla, O. Study of diatoms/aqueous solution interface. I. Acid-base equilibria, surface charge and spectroscopic observation of two freshwater peryphytic and two marine planctonic diatoms. *Geochim. Cosmochim. Acta* **2004**, *68*, 4039–4058.
(14) Pokrovsky, O. S.; Viers, J.; Emnova, E. E.; Kompantseva, E. I.; Freydier, R. Copper isotope fractionation during its adsorption on soil and aquatic bacteria and metal hydroxides: possible structural control. *Geochim. Cosmochim. Acta* **2008**, *72*, 1742–1757.
(15) Allison, J. D.; Brown D. S.; Novo-Gradac, K. J. *MINTEQA2/PRODEFA2, A geochemical assessment model for environmental systems: Version 3.0 user's manual*; U.S. EPA: Athens, GA, 1991.
(16) Knauer, K.; Behra, R.; Sigg, L. Effects of free Cu^{2+} and Zn^{2+} ions on growth and metal accumulation in freshwater algae. *Environ. Toxicol. Chem.* **1997**, *16*, 220–229.
(17) Le Faucheur, S.; Behra, R.; Sigg, L. Thiol and metal contents in periphyton exposed to elevated copper and zinc concentrations: a field and microcosm study. *Environ. Sci. Technol.* **2005**, *39*, 8099–8107.
(18) Hudson, R. J. M.; Morel, F. M. M. Distinguishing between extracellular and intracellular iron in marine phytoplankton. *Limnol. Oceanogr.* **1989**, *34*, 1113–1120.
(19) Pokrovsky, O. S.; Pokrovski, G. S.; Schott, J.; Galy, A. Germanium adsorption on goethite and Ge coprecipitation with iron hydroxide: X-ray Absorption Spectroscopy (XAS) study and macroscopic characterization. *Geochim. Cosmochim. Acta* **2006**, *70*, 3325–3341.
(20) Pokrovsky, O. S.; Martinez, R.; Golubev, S. V.; Kompantseva, E. I.; Shirokova, L. S.; Adsorption of metals and protons on *Gloeocapsa* sp. cyanobacteria: a surface speciation approach. *Appl. Geochem.*; **2008**, in press. doi:10.1016/j.apgeochem.2008.05.007.
(21) Gélabert, A.; Pokrovsky, O. S.; Schott, J.; Boudou, A.; Feurtet-Mazel, A. Cadmium and lead interaction with diatom surfaces: a combined thermodynamic and kinetic approach. *Geochim. Cosmochim. Acta* **2007**, *71*, 3698–3716.
(22) Gonzalez-Davila, M. The role of phytoplankton cell on the control of heavy metal concentrations in seawater. *Mar. Chem.* **1995**, *48*, 215–236.
(23) Toner, B.; Manceau, A.; Marcus, M. A.; Millet, D. B.; Sposito, G. Zinc sorption by a bacterial Biofilm. *Environ. Sci. Technol.* **2005**, *39*, 8288–8294.
(24) Xia, H.; Rayson, G. D. ^{113}Cd-NMR spectrometry of Cd^{2+} binding sites on algae and higher plant tissues. *Adv. Environ. Res* **2002**, *7*, 157–167.
(25) Carrilho, E. M.; Ferreira, A. G.; Gilbert, T. Characterization of sorption sites on *Pilayella littoralis* and metal binding assessment using ^{113}Cd and ^{27}Al nuclear magnetic resonance. *Environ. Sci. Technol.* **2002**, *36*, 2003–2007.
(26) Le Faucheur, S.; Behra, R.; Sigg, L. Phytochelatin induction, cadmium accumulation and algal sensitivity to free cadmium ion in *Scenedesmus vacuolatus*. *Environ. Toxicol. Chem.* **2005**, *24*, 1731–1737.
(27) Le Faucheur, S.; Schildknecht, F.; Behra, R.; Sigg, L. Thiols in *Scenedesmus vacuolatus* upon exposure to metals and metalloids. *Aquat. Toxicol.* **2006**, *80*, 355–361.
(28) Lee, J.; Ahner, B.; Morel, F. M. M. Export of cadmium and phytochelatin by the marine diatom *Thalassiosira weissflogii*. *Environ. Sci. Technol.* **1996**, *30*, 1814–1821.
(29) Morelli, E.; Scarano, G. Synthesis and stability of phytochelatins induced by cadmium and lead in the marine diatom Phaedactylum tricornutum. *Mar. Environ. Res.* **2001**, *52*, 383–395.
(30) Mishra, B.; Fein, J. B.; Boyanov, M. I.; Kelly, S. D.; Kemner, K. M.; Bunker, B. A. Comparison of Cd Binding Mechanisms by Gram-Positive, Gram-Negative and Consortia of Bacteria Using XAFS. *AIP Conf. Proc.* **2007**, *882*, 343–345; DOI: 10.1063/1.2644520, X-RAY Absorption Fine Structure - XAFS13; February 2.
(31) Guiné, V.; Spadini, L.; Muris, M.; Sarret, G.; Delolme, C.; Gaudet, J.-P.; Martins, J. M. F. Zinc sorption to cell wall components of three Gram-negative bacteria: a combined titration, modeling and EXAFS study. *Environ. Sci. Technol.* **2006**, *40*, 1806–1813.
(32) Henkel, G.; Krebs, B. Metallothioneins: zinc, cadmium, mercury, and copper thiolates and selenolates mimicking protein active site features - structural aspects and biological implications. *Chem. Rev.* **2004**, *104*, 801–824.
(33) Blanc, G.; Schäfer, J. ; Audry, S.; Robert, S.; Bossy, C. ; Lavaux, G.; Luissalde, J. P.; Maneux, E. La ballade du cadmium dans le système Lot-Garonne-Gironde: flux naturels et anthropisation. In *Système fluvio-estuarien de la Gironde*; GIS ECOBAG: Toulouse, France, 2006; pp 14−20.
(34) Duong, T. T. Réponses des diatomées fixées aux pollutions organiques et métalliques dans les hydrosystèmes Nhue-Tolich (Hanoi, Vietnam) et Lot-Riou-Mort (France), PhD thesis, Univ. Bordeaux 1, Ecole Doctorale des Sciences du Vivant, Géosciences et Sciences de l'Environnement,2006; p 175.
(35) Newville, M. IFEFFIT: interactive XAFS analysis and FEFF fitting. *J. Synchrotron. Radiat.* **2001**, *8*, 322–324.

ES800521A